First European Conference on Earthquake Engineering and Seismology
(a joint event of the 13th ECEE & 30th General Assembly of the ESC)
Geneva, Switzerland, 3-8 September 2006
Paper Number: 1424

MODELLING DIRECTIVITY EFFECTS OF THE OCTOBER 31, 2002 (M_W=5.8), MOLISE, SOUTHERN ITALY, EARTHQUAKE.

Gianlorenzo FRANCESCHINA[1], Francesca PACOR[1], Giovanna CULTRERA[2], Antonio EMOLO[3] and Frantisek GALLOVIC[4]

SUMMARY

Acceleration time series recorded by the Italian Strong Motion Network (RAN) during the October 31, 2002 (Mw=5.8), Molise earthquake, are employed in order to investigate source effects on the ground motion in the epicentral area. We consider two different seismogenic sources: a fault model inferred from inversion of teleseismic, regional and local seismic signals [Vallée and Di Luccio, 2005], and a fault model based on seismotectonic data [Basili and Vannoli, 2005].

Both source studies suggest a deep location of the earthquake fault plane (ranging from 6.0 to 20.1 km and from 12.0 to 19.9 km, respectively), however, with considerably different fault lengths (5.2 and 10.5 km, respectively), and widths (14.2 and 8 km, respectively). Due to these differences, only the second model allows for effective horizontal unilateral rupture propagation.

Finite fault effects are modelled by the Deterministic-Stochastic-Method (DSM) [Pacor et al., 2005], and the Hybrid Integral-Composite source model (HIC) [Gallovic and Brokesova, 2006]. In both methods k-square slip distributions on the faults are considered.

We simulate the October 31, 2002 earthquake considering: 1) Vallée and Di Luccio [2005] faultwith a bilateral rupture propagation, and 2) Basili and Vannoli [2005] fault with unilateral directions of the rupture propagation. The spectral attenuation is modelled using a regional estimate of the quality factor [Castro et al., 2004] and *k* values estimated from acceleration records. Comparison between synthetic and recorded data at nearby stations (hypocentral distances < 60 km) performed in terms of frequency content and peak ground motion, favours the model with unilateral propagation of the rupture.

Assuming the source model with unilateral rupture propagation, we utilize both asymptotic and full wave field methods in order to simulate ground shaking scenarios for an area extending up to 150 km epicentral distance. These results are then subjected to comparison with peak ground accelerations recorded in the far field.

[1] Istituto Nazionale di Geofisica e Vulcanologia – Sezione di Milano, via Bassini,15, Milano, Italy.
Email : glf@ingv.mi.it ; pacor@ingv.mi.it
[2] Istituto Nazionale di Geofisica e Vulcanologia – Sezione di Roma 1. via di Vigna Murata, 605, Roma, Italy.
Email : cultrera@ingv.it
[3] Dipartimento di Scienze Fisiche, Universita' degli Studi ''Federico II'', Complesso Universitario di Monte S.Angelo, via Cintia, Napoli, Italy. Email : antonio.emolo@na.infn.it
[4] Department of Geophysics, Faculty of Mathematics and Physics, Charles University, V Holesovickach 2, Praha, Czech Republic.
Email : gallovic@karel.troja.mff.cuni.cz

1. INTRODUCTION

On October 31 (10:32 UTC) and November 1 (15:08 UTC), 2002, two moderate earthquakes (Mw=5.8 and Mw=5.7, respectively) struck the Molise (Southern Italy) region killing young human lives in a school collapse. The earthquakes caused also moderate damage in an area comprising 29 municipalities, with a total population of about 150,000 inhabitants [Maffei and Bazzurro, 2004; Nuti et al., 2004]. Main shocks sources were located at about 20 km depth, on a deep seismogenic structure underlying the Apulia Platform [Valensise et al., 2004]. Seismicity was detected at corresponding depths by a temporary seismic network, installed soon after the first main event [Chiarabba et al., 2005]. More than 1900 aftershocks, located with errors lower than 0.5 km, revealed an east-west-trending nearly vertical buried structure extending from 10 to 25 km depth composed of two 15 km long main segments. For this twin earthquake, two different couples of seismogenic sources were proposed. Based on inversion of teleseismic, regional and local seismic signals, Vallée and Di Luccio [2005] modelled the first event by a 5.2 x 14.2 km^2 fault plane extending from 6.0 to 20.1 km depth, and the second one by a 8.6 x 9.7 km^2 fault with depths ranging from 9.0 to 18.4 km. A fault model based on seismotectonic data [Basili and Vannoli, 2005] hypothesizes a similar fault for this second shock. However, this model associates the first event with a 10.5 x 8.0 km^2 fault extending from 12 to 19.9 km depth. Hereafter, we denote as VDL31, BV31, VDL01 and BV01 the fault models of Vallée and Di Luccio [2005] and Basili and Vannoli [2005] for the October, 31 and November, 1, 2002, earthquakes, respectively.

Accelerometric data recorded by the Italian Strong Motion Network (RAN), show a strong anisotropy in PGA distribution associated with the October, 31 main shock [Gorini et al., 2004]. The closest stations, located approximately at the same epicentral distances but to the east and west from the source, exhibit strong differences in the ground shaking level with PGA ratios up to 10. Since similar differences are not observed for the second main shock, we hypothesize that directivity effect could be responsible for the WE trending anisotropy of the ground motion recorded during the first event. It is noteworthy that, for the first shock, fault lengths and widths proposed by the adopted source models are considerably different (5.2 and 10.5 km, for VDL31 and BV31 fault lengths, respectively). As a consequence, only BV31 model allows for effective horizontal unilateral rupture propagation. In this work we investigate directivity properties of the October 31 event by comparison of acceleration data recorded at nearby stations (hypocentral distances < 60 km) with synthetics obtained by the Deterministic-Stochastic Method by Pacor et al. [2005]. Comparison is performed in terms of frequency content and peak ground accelerations. We utilize the Deterministic-Stochastic Method and a broadband simulation method, the Hybrid Integral-Composite k-squared Source Model introduced by Gallovic and Brokesova [2006], in order to simulate the ground motion up to 150 km epicentral distance. These results are then subjected to comparison with peak ground accelerations recorded in the far field.

2. DATASET

The October 31 and November 1, 2002, events were recorded by 12 and 11 accelerometric stations, respectively. The dataset consists of accelerograms recorded from both digital and analog instruments, at hypocentral distances ranging between 28 and 195 km (Fig. 1 and Table 1). Digital instruments are Kinemetric 19-24 bits data logger equipped with three component sensors (Kinemetric Episensor) with +/- 1g full scale. Analog instruments are three components Kinemetric SMA1 and Teledyne RFT250 with +/- 1g full scale, except for San Severo (SSV) station, whose full scale was set to +/-0.25 g. For all records the sampling frequency is 200 Hz [SSN, 2004]. Data from analog instrument were base-line corrected, de-convolved with the instrument response and band-pass filtered. Data from digital instrument were base-line corrected and band-pass filtered. High- and low-pass filter frequencies for data correction were chosen according to the signal-to-noise ratio and to the natural frequency of the sensor, respectively. After correction, the available frequency band generally ranges between 0.2 Hz and the instrument natural frequency (from 13 to 26 Hz for analog and about 50 Hz for digital instruments).

Acceleration time series recorded at nearby stations (hypocentral distances < 60 km) show high variability in both amplitude and duration (Fig.2), with PGAs ranging between 4.9 to 61.3 gal and durations (measured as the time interval during which the squared acceleration rises from 5 to 75% of its maximum value) between 4 and 20 s. As regard the directivity, stations located eastward from the sources (namely LSN, SSV and SNN) and stations located westward (CMM, GLD and VSE) are particularly relevant. These are characterized by different soil categories but, unfortunately, two of them did not record both events. However, it is noteworthy that CMM and SNN, both classified as “Rock” and located at similar distances, recorded the first event with different levels of shaking (mean horizontal PGAs being 36.0 and 6.2 gal for SNN and CMM, respectively). Moreover, the second main shock produced PGA values at westward sites (particularly CMM and GLD) comparable to the first shock

but lower values at SSV (mean horizontal PGAs being 54.1 and 22.7 gal for the first and the second shock, respectively).

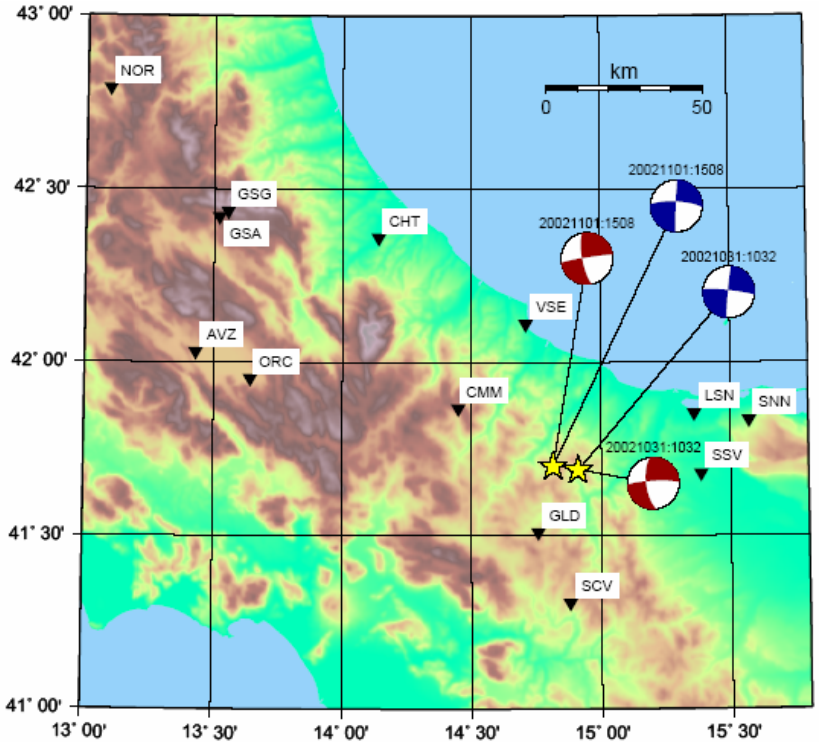

Figure 1: Accelerometric stations that recorded the October 31 and November 1, 2002, Molise (Southern Italy) earthquakes. Epicenter locations are from Vallée and Di Luccio [2005]. "Blue" and "red" focal mechanisms are taken from Vallée and Di Luccio [2005] and Basili and Vannoli [2005] models, respectively.

Table 1: Acceleration data of the October 31 and November 1, 2002, Molise (Southern Italy) earthquakes. Soil: site geology according to the National Seismic Survey of Italy (SSN) classification; I: instrument type (A=analog, D=digital); R: hypocentral distance according to Chiarabba et al., [2005]; pga [NS] and pga [EW] : corrected peak ground accelerations of North-South and East-West components, respectively; k and σ_k : mean diminution parameter and its standard deviation, respectively, estimated from horizontal components of recordings of the two October-November main shocks.

Code	Station name	Soil	I	October 31, 2002, M_W=5.8			November 1, 2002, M_W=5.7			k	σ_k
				R [km]	pga [NS] [gal]	pga[EW] [gal]	R [km]	pga [NS] [gal]	pga[EW] [gal]	[s]	[s]
AVZ	Avezzano	Stiff	D	130.4	6.7	3.7	122.9	3.2	3.7	0.1700	0.0024
CHT	Chieti	Soft	D	100.5	5.7	6.7	95.2	7.9	7.6	0.0775	0.0009
CMM	Castiglione M. Marino	Rock	D	48.5	4.9	7.9	41.3	5.6	7.0	0.0555	0.0006
GLD	Gildone	Stiff	A	32.5	12.1	17.6	28.1	17.1	18.3	0.0625	0.0014
GSA	Gran Sasso Assergi	Stiff	D	142.5	1.3	1.2	136.0	1.2	1.2	0.0580	0.0006
GSG	Gran Sasso Laboratorio	Rock	D	141.2	0.3	0.2	134.9	0.3	0.2	0.0517	0.0004
LSN	Lesina	Soft	A	47.2	58.4	62.1	-	-	-	0.0410	0.0013
NOR	Norcia	Stiff	D	194.5	1.4	1.8	188.5	1.0	1.6	0.1232	0.0027
ORC	Ortucchio	Rock	D	111.5	3.7	4.0	103.9	3.0	3.1	0.0700	0.0009
SCV	S. Marco dei Cavoti	Stiff	D	-	-	-	47.0	4.6	4.4	0.0695	0.0009
SSV	San Severo	Soft	A	45.5	61.3	47.8	50.8	25.7	20.0	0.0220	0.0013
SNN	Sannicandro Garganico	Rock	A	61.5	37.3	34.7	-	-	-	0.0330	0.0055
VSE	Vasto Europa	Stiff	A	54.4	17.6	42.0	51.3	15.6	33.4	0.0447	0.0021

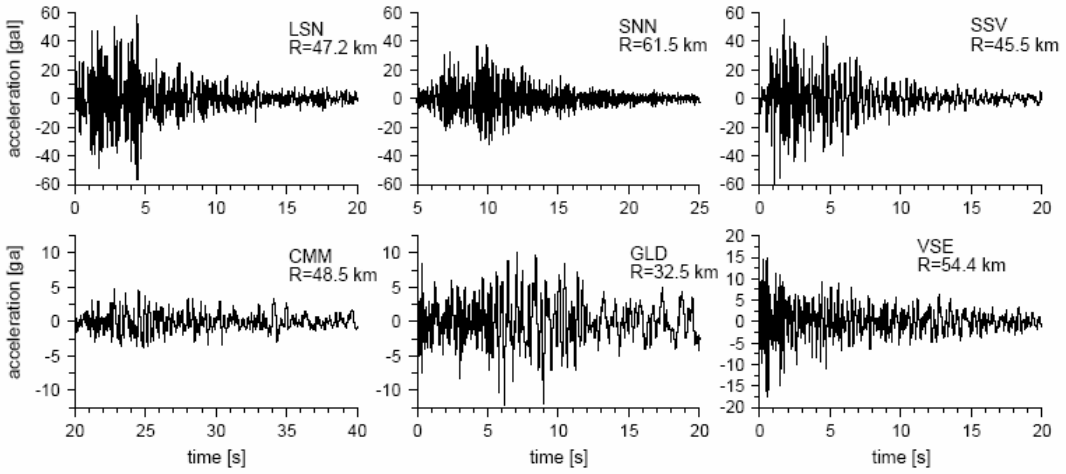

Figure 2: NS component acceleration time series recorded during the October 31, 2002 Molise earthquake at stations with hypocentral distance < 60 km. Note the different amplitude scales used for eastward (top panels) and westward (bottom panels) stations.

3. MODELLING METHODS

Two hybrid stochastic-deterministic numerical methods have been adopted for simulating strong ground motion in the Molise area: the Deterministic-Stochastic Method of Pacor et al. [2005] (hereafter referred to as DSM), and the Hybrid Integral-Composite k-squared source model by Gallovic and Brokesova [2006] (hereafter referred to as HIC). The adopted simulation techniques take into account finite fault effects considering a radial rupture propagation with constant rupture velocity and heterogeneous final slip distribution. Seismic waves are propagated through a crustal 1D velocity model. Spectral attenuation model is also taken into account. Both methods allow effective simulations although specifying only a relatively small number of input parameters, representing average properties of seismic source and waves propagation.

3.1 Deterministic-Stochastic Method (DSM)

DSM is a modification of the stochastic point source simulation method of Boore [2003], accounting for finite fault effects by a simplified formulation of the isochron theory [Bernard and Madariaga, 1984; Spudich and Frazer, 1984]. Schematically, the synthesis of a time series is a four-step procedure consisting of:

A) Computation of the deterministic acceleration envelope of shear waves radiated from an extended fault. For this purpose, a simplified formulation of the representation theorem by means of the isochron theory is solved for a given kinematic rupture process. The rupture model is described by specifying a nucleation point on the fault plane, from which the rupture propagates radially outward with a prescribed rupture velocity, and the final slip distribution. The Green functions are computed as asymptotic solution of the elastodynamic equation (ray theory) in a flat-layered velocity model.

B) Generation and windowing of the white noise time-sequence. DSM method accounts for stochastic properties of the acceleration ground motion by generating time series of Gaussian white noise. The noise time-sequence is then windowed with the acceleration envelope computed previously (in step A).

C) Introduction of the point-source-like reference spectrum. The windowed-noise time sequence is transformed into the frequency domain and multiplied with point-source-like amplitude spectrum$A(\omega,R) = \omega^2$ C G(R) $S(\omega)$ $A_P(\omega,R)$, where ω represents the angular frequency and R is the average source-to-site distance, computed through the isochron theory. C is a constant including the free surface amplification factor (Fs = 2), the average radiation pattern for S waves ($R_{0\varphi}$ = 0.63), the energy partitioning factor between the two horizontal components of the motion (V=0.707) and the density and S wave velocity at source (ρ=2.8 g/cm^3 and β=3.5 km/s, respectively). G(R) is the geometrical spreading factor, $A_P(\omega, R)$ stands for attenuation model $A_P(\omega,R) = \exp(-\omega R / 2\beta Q(\omega)) \exp(-\omega k / 2)$, specified in terms of quality factor $Q(\omega)$ and diminution parameter k [Anderson and Hough, 1984]. Source term $S(\omega)$ is characterized by a ω–square model described by seismic moment, M_0, and apparent angular corner frequency, ω_a , proportional to the inverse of the apparent rupture duration as

perceived by the observer. Note that in this way site-to-site variations of ω_a produce a spectrum modified by directivity effects, as observed in the near-field ground motion.

D). Transformation back to the time domain of the complex acceleration Fourier spectrum.

Application of steps from A) to D) implies that the resulting acceleration time series involves stochastic properties of the adopted Gaussian white noise and deterministic properties of the acceleration envelopes and point-source-like reference spectra (obtained by means of the kinematic finite-fault source modeling) .

3.2 Hybrid Integral-Composite method (HIC)

In this model the faulting process is decomposed into slipping on individual, formal, overlapping subsources of various sizes, distributed randomly along the fault. A subsources database is first built, including the subsources' positions on the fault, their dimensions, mean slips (and consequently seismic moments) and corner frequencies. Subsource dimensions are taken as integer fractions of fault's length and width. Scaling properties of the subsources are the same as used by Zeng et al. [1994]. Their number-size distribution obeys a power law with fractal dimension D=2 and their mean slips are proportional to their dimensions (so-called constant stress-drop scaling). The subsource's scaling implies that the subsources compose k-square slip distribution [Andrews, 1980]. Note that although such a decomposition is inherent to the composite approaches, in the employed hybrid model the same set of subsources is used both in the integral (low-frequency) and composite (high-frequency) calculations.
More specifically, in the low-frequency range, the computation is performed according to the well-known representation theorem. We discretize the fault densely enough to evaluate the representation integral correctly up to a certain frequency. The static slip at a point is given by the sum of static slips of all the subsources from the database that contain the point (assuming a k-squared slip distribution on each individual subsource). The rupture time is given by the distance of the point from the nucleation point assuming constant rupture velocity. The slip function is assumed to be a smoothed ramp with constant rise time. As regards the high-frequency range, the subsources from the database are treated as individual point sources with Brune's source time function. Their seismic moments and corner frequencies are obtained directly from the database. The rupture time is given by the time the rupture needs to reach the subsource's center (assuming the same constant velocity as for the integral approach). In the cross-over frequency range we apply weighted averaging of the integral and composite parts of the spectrum. Let us emphasize that this approach provides particular frequency dependent directivity effect: while at low frequencies the wavefield is coherent due to evaluation of the representation integral, at high frequencies the wave-field contributions sum incoherently due to the random subsources positions and, therefore, the directivity effect vanishes. For more detailed explanation see Gallovic and Brokesova [2006].
As such, the method can be combined with any technique yielding Green's functions. In this paper we utilize the discrete wave-numbers method [Bouchon, 1981].

4. MODELLING DETAILS

Table 2 summarizes the source parameters adopted for simulation of the October 31, 2002, event. We consider VDL31 and BV31 source geometries with nucleation points constrained by the epicenter location. As a consequence, only BV31 model implies WE unilateral rupture propagation. Seismic moment is inferred from the moment magnitude considered and average slips are computed assuming $\mu=3.6\text{x}10^{11}$ dyne/cm^2. Both models are compatible with Wells and Coppersmith [1994] relationships relating moment magnitude to rupture area. A constant rupture velocity of 2.8 km/s (corresponding to $0.8V_S$) is assumed in all simulations.
For both models, k-square slip distributions are assumed. They come from the HIC model, i.e. from a random realization of the subsources distribution. To introduce an asperity in the center of the fault, the position of the largest subsources is imposed. Figure 3 shows the surface projections of the assumed faults and the adopted slip models. The crustal model is taken from Vallée and Di Luccio [2005]. The spectral attenuation model $A_P(\omega,R)$ involves $Q(f) = 31.5\ f^{1.7}$ [Castro et al., 2004], and site dependent diminution parameter k, estimated using horizontal components recorded during the October and November main events. A suitable frequency band (depending on quality of data, generally ranging from 3-4 Hz to 20-25 Hz) was chosen in order to perform a reliable regression. Figure 4 shows some examples of k estimates and Table 1 summarizes the results. The k estimates are generally characterized by low uncertainties (relative errors are of the order of a few percent). Except for SSV, the well-defined linear decay allows for stable regressions, generally independent of slight changes of the adopted frequency band.

Table 2: Source parameters adopted for simulation of the October 31, 2002, Molise earthquake, according to Vallée and Di Luccio [2005] (VDL31) and Basili and Vannoli [2005] (BV31). M_W : moment magnitude; M0 : seismic moment ; Δu : average slip ; L and W : source dimentions; φ, δ and λ: strike, dip and rake; Z_{TOP} : top depth.

	M_W	$M_0[10^{17}Nm]$	Δu [cm]	L x W [km^2]	φ[°]	δ[°]	λ[°]	Z_{TOP} [km]
VDL31	5.8	5.5	25	5.2 x 14.2	276	84	-177	6.0
BV31	5.8	5.5	20	10.5 x 8.0	267	82	-157	12.0

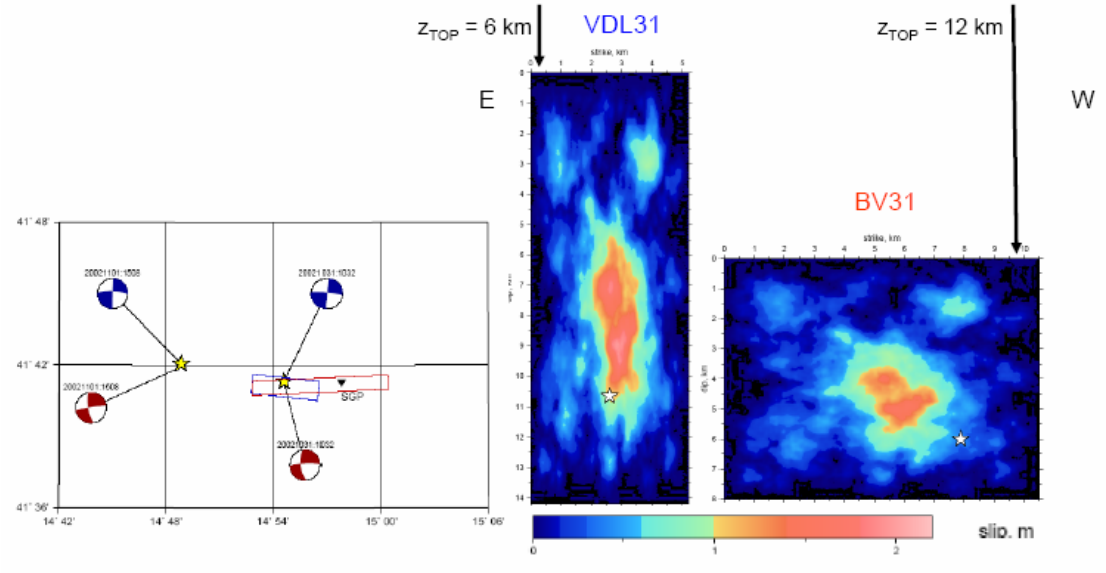

Figure 3: Fault surface projections (left) and slip distributions (right) adopted for the October 31, 2002, Molise main shock. Blue and red symbols represent VDL31 and BV31 fault models, respectively. Yellow stars mark surface projections of nucleation points corresponding to hypocenter locations (white stars on right panels). Location and focal mechanisms of the November 1, 2002, and location of S.Giuliano di Puglia (SGP) are also shown.

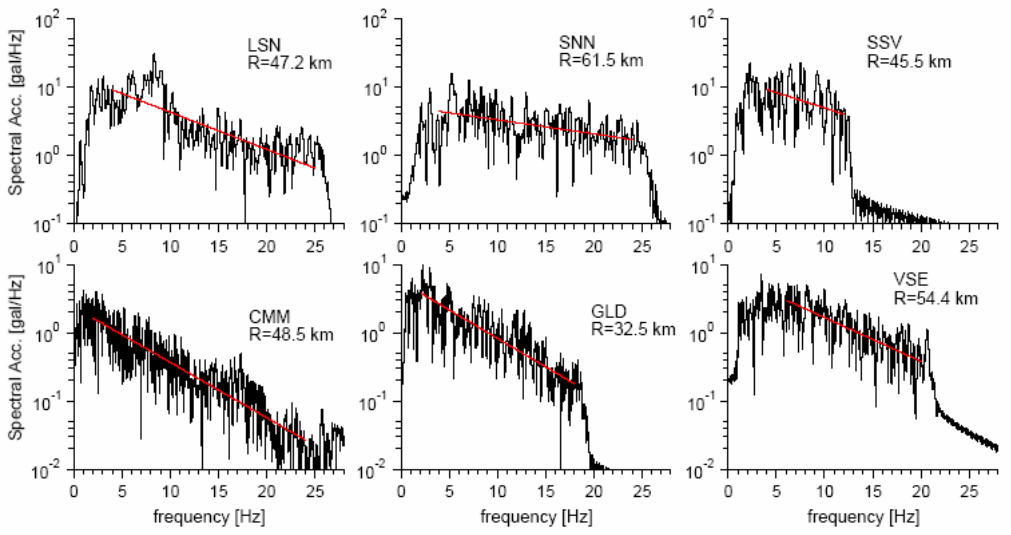

Figure 4: Estimates of *k* from acceleration NS components recorded during the October 31 main shock at stations CMM, GLD, VSE, LSN, SNN and SSV. Frequency bandwidths for regressions were chosen according to the corner frequency of the event and the high frequency noise of data.

5. RESULTS AND DISCUSSION

As previously mentioned, a combined effect of site amplification and directivity can be supposed to explain the observed differences between eastward and westward stations in the October/November 2002 Molise earthquakes. Comparison of synthetic and recorded acceleration amplitude Fourier spectra at nearby stations (hypocentral distance < 60 km) is shown in Figure 5 for DSM simulations. Some of the stations show amplification in specific frequency bands probably due to site effects (see, e.g., LSN between 5 and 10 Hz). However, the eastward stations (LSN, SNN, SSV) are generally characterized by higher spectral levels with respect to the westward ones (GLD, CMM, VSE). Since high frequency spectral level obtained through DSM simulations depends on the corner frequency squared, eastward sites show higher synthetic spectral accelerations than westward sites when BV31 model is adopted. Especially for eastward sites, BV31 model produces a better fit with recorded data than VDL31 model.

Acceleration spectra recorded at westward sites are instead equally well fitted with VDL31 and BV31 models, with a possible exception of GLD spectrum which is better fitted with the second model in the lower frequency band (f < 2 Hz). In fact, in comparison between recorded and simulated spectra, average site amplification factors ranging between 1.5 and 4.0 should be considered for these stations (see H/V spectral ratios in [Gorini et al., 2004]). It is noticeable that VSE distance and back-azimuth involve identical DSM simulations with VDL31 and BV31 models. PGAs simulated by DSM are compared with recorded PGAs in Table 3. Stations GLD, SSV and SSN show the best agreement between recorded and synthetic data obtained by BV31 model. For the other stations synthetic data do not fit the observed peaks so well. However, BV31 model shows again a better fit than VDL31 model. Global comparison of DSM simulations performed at nearby stations thus favours a unilateral propagation of the rupture of the October 1, 2002 main shock.

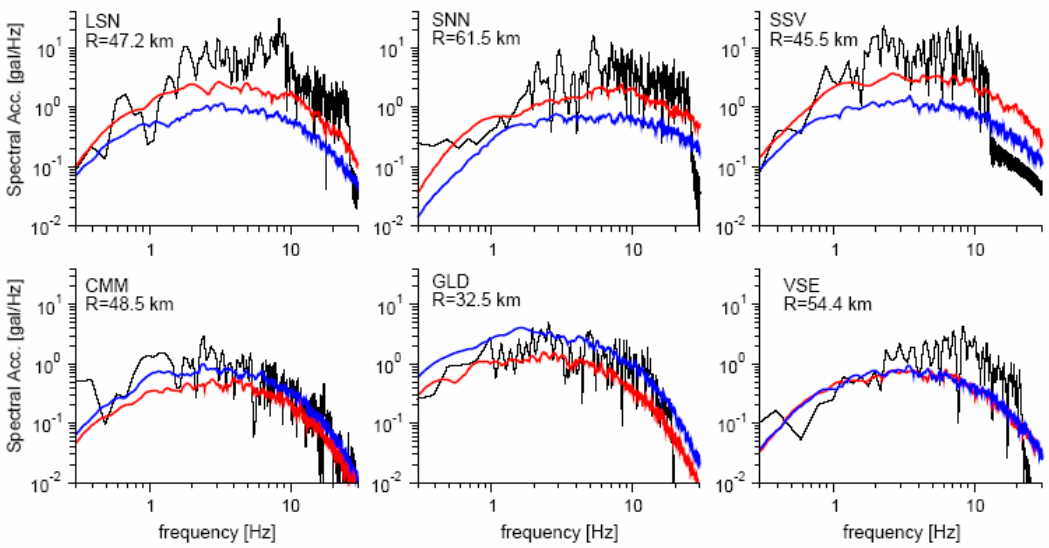

Figure 5: Comparison between DSM synthetic (coloured lines) and recorded (black lines) acceleration spectra of the October 1 main event (NS components) at stations CMM, GLD, VSE, LSN, SNN and SSV. Blue and red lines refer to VDL31 and BV31 models, respectively.

Table 3: PGAs obtained by DSM simulations with BV31 and VDL31 models compared with recorded PGAs at nearby stations. R: hypocentral distance according to Chiarabba et al., [2005]; pga [EW], pga [NS] and pga[MH]: recorded and simulated peak ground accelerations of East-West, North-South and Mean Horizontal components, respectively.

Code	Station name	Distance	Acceleration data			BV31	VDL31
		R [km]	pga [EW] [gal]	pga [NS] [gal]	pga[MH] [gal]	pga[MH] [gal]	pga[MH] [gal]
CMM	Castiglione M. Marino	48.5	7.9	4.9	6.2	4.9	7.3
GLD	Gildone	32.5	17.6	12.1	14.6	10.5	28.7
LSN	Lesina	47.2	62.1	58.4	60.2	34.1	12.2
SSV	San Severo	45.5	47.8	61.3	54.1	51.8	14.3
SNN	Sannicandro Garganico	61.5	34.7	37.3	36.0	38.1	12.6
VSE	Vasto Europa	54.4	42.0	17.6	27.2	9.2	7.4

BV31 model is adopted to simulate the ground shaking up to 150 km epicentral distance. Simulations are performed by DSM at grid points regularly spaced of 10 km and by HIC at sparse points located at sites corresponding to accelerometric stations. Figure 6 shows the PGA distribution obtained by DSM. Ground acceleration reflects directivity properties of the source. However, due to the assumed fault depth, directivity does not produce elongated shapes of strong ground shaking but it only shifts the position of the maximum shaking area respect to the epicentre, slightly altering the circular symmetry of PGA distribution. PGA attenuation with fault distance is shown in Figure 7, where recorded data are also shown for comparison. Continuous curves are obtained by averaging DSM simulations over all azimuths. Synthetic peaks follow the same general trend of recorded PGAs. Except for VSE, nearby stations (fault distance < 50 km), show recorded peaks in accordance with the above-mentioned directivity features. Westward sites are characterized by PGAs lower than mean simulated peaks. Eastward sites display an opposite trend, probably enhanced by site effects. At fault distances > 50 km, propagation effects are dominant and produce high variability in the recorded ground motion. Nevertheless, simulated PGAs follow the general trend of data up to 150 km fault distance.
HIC simulations are compared with recorded data in term of horizontal PGAs in Figure 7 and amplitude Fourier spectra in Figure 8. Except for LSN, SSV (EW component) and GSG, simulated peaks are in relatively good agreement with recorded ones. According to H/V spectral ratios performed by Gorini et al. [2004], LSN station is affected by a strong site effect (up to 4-5 amplification factor between 5 and 10 Hz). PGAs simulated by HIC are also in agreement with mean values computed by DSM between 20 and 150 km fault distance.
As regards the simulated and recorded spectra comparison at nearby stations (Figure 8), with the exception of LSN, we can observe a general agreement at high frequencies (where HIC method adopt a composite simulation model) and at low frequencies (f < 1 Hz) for westward stations. For eastward stations, at low frequencies the fit is not so good, but it is noticeable that only CMM station is equipped with a digital instrument and that analog data are generally affected by large uncertainties in this range of frequencies.

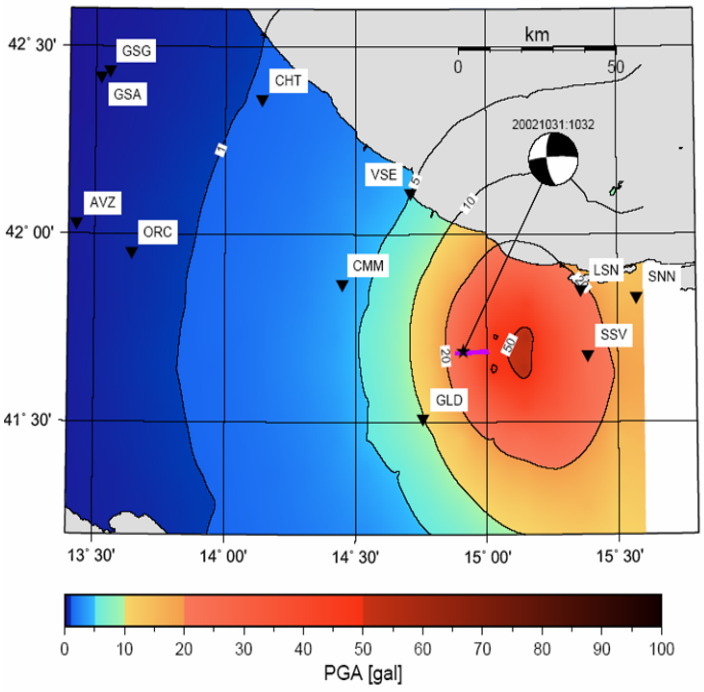

Figure 6: PGA distribution obtained by DSM with BV31 model.

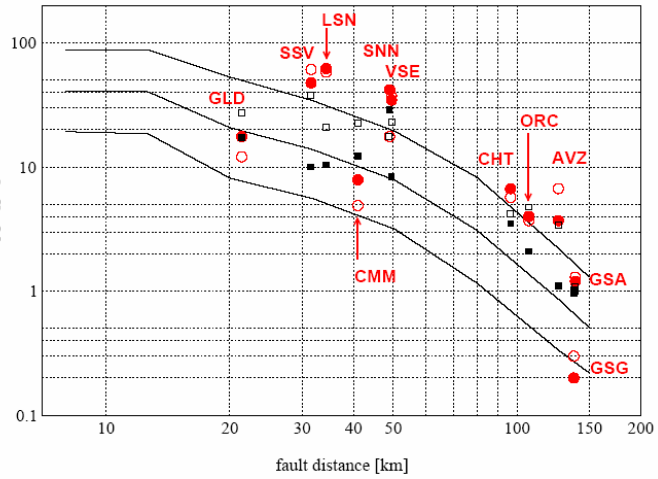

Figure 7: PGA attenuation obtained by DSM and by HIC with BV31 model: continuous lines refer to mean and mean ± 1 standard deviation simulated by DSM at equally spaced points up to 150 km fault distance; black dots are HIC simulations at accelerometric stations. Recorded PGAs (red dots) are also shown for comparison. Open and close dots represent NS and EW components, respectively.

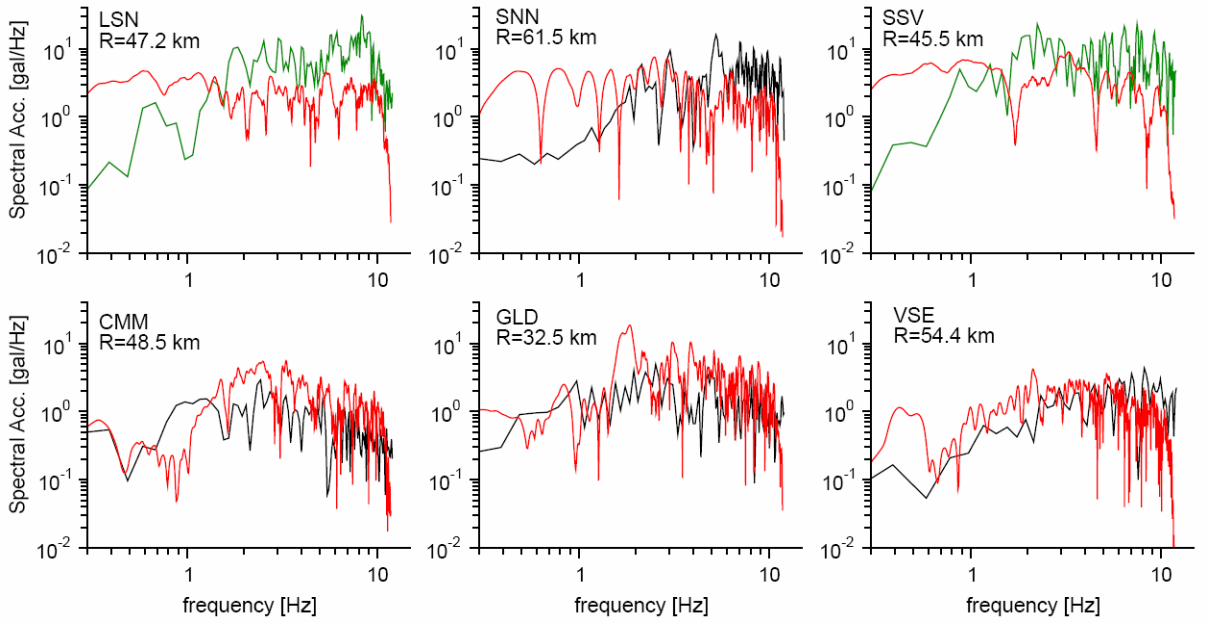

Figure 8: Comparison between HIC synthetic (red lines) and recorded (black and green lines) acceleration spectra of the October 1, 2002 event, at stations CMM, GLD, VSE, LSN, SNN and SSV. Green curves are acceleration spectra recorded at soft soil stations. Comparison is made up to the highest frequency simulated by HIC (12 Hz), for NS component.

6. CONCLUSIONS

Two hybrid stochastic-deterministic numerical methods were employed to compute ground shaking scenarios for the October 31, 2002 Molise (M_W=5.8) earthquake: the Deterministic-Stochastic Method (DSM) by Pacor et al. [2005], and the Hybrid k-squared Source Model (HIC) introduced by Gallovic and Brokesova [2006]. Simulations were performed based on two different hypothesis of seismic source: model VDL31, inferred from inversion of teleseismic, regional and local seismic signals, and model BV31, inferred from seismotectonic data. Both models approximately suggest the same rupture area (about 80 km^2) and nucleation point, however, with considerably different fault lengths (5.2 and 10.5 km, respectively). As a consequence, only BV31 allows for effective horizontal unilateral propagation. We investigate directivity properties of the October 31 event by comparison of acceleration data recorded at nearby stations (hypocentral distances < 60 km) with synthetics obtained by DSM. Afterwards, we adopted both DSM and HIC in order to simulate the ground motion up to 150 km epicentral distance.

Comparison between synthetic and recorded acceleration spectra performed at nearby stations shows that, especially for eastward sites, BV31 model produces a better fit with recorded data than VDL31 model, while acceleration spectra recorded at westward sites are equally well fitted with VDL31 and BV31 models. Also comparison between synthetic and recorded peak ground accelerations is generally better for BV31 than VDL31. Therefore, DSM simulations performed at nearby stations, favours a unilateral propagation of the rupture of the October 1, 2002 main shock.

It is noteworthy that site effects were not included in the abovementioned comparison and that, according to Gorini et al.[2004], nearby stations could be affected by average site amplification factors ranging between 1.5 and 4.0. The crustal model is also very simple, and with this respect, the obtained fit is relatively good.

Synthetic peaks obtained by DSM and HIC simulations up to 150 km epicentral distance, follow the same general trend of recorded PGAs, with recorded peaks in accordance with the above-mentioned directivity features at nearby stations. A proper inclusion of site effects could also improve the fit between simulated and recorded peaks at large distances.

As regard to HIC synthetics, the observations have lower difference between NS and EW peak accelerations. This could be perhaps addressed to vanishing radiation pattern at high frequencies (see Satoh [2002]), and it will be implemented in the future in HIC

Acknowledgements: The research was supported by DPC-INGV 2004-2006 convention (S3 Project)

7. REFERENCES

Anderson, J.G. and Hough, S. (1984), A model for the shape of Fourier amplitude spectrum of acceleration at high frequencies, *Bull. Seism. Soc. Am.*, **74**, 1969-1994.

Andrews, D. J. (1980), A stochastic fault model, 1. Static case, *J. Geophys. Res.*, **85**, 3867-3877.

Bernard, P. and Madariaga, R. (1984), A new asymptotic method for the modeling of near field accelerograms, *Bull. Seism. Soc. Am.*, **74**, 539-558.

Bouchon, M. (1981), A simple method to calculate Green's functions for elastic layered media, *Bull. Seism. Soc. Am.*, **71**, 959-971.

Castro, R. R., Gallipoli, M. R. and Mucciarelli, M. (2004), An attenuation study in Southern Italy using local and regional earthquakes recorded by seismic network of Basilicata, *Ann .Geophys .*, **47**, 1597-1608.

Gallovic, F. and Brokesova, J. (2006), Hybrid k-squared Source Model for Strong Ground Motion Simulations: an Introduction, submitted to *Physics .Earth. Planet. Int.* (http://geo.mff.cuni.cz/~gallovic)

Chiarabba, C, De Gori, P., Chiaraluce, L. Bordoni, P., Cattaneo, M., De Martin, M., Frepoli, A., Michelini, A., Monachesi, G., Moretti, M., Augliera, P., D'Alema, E., Frapiccini, M., Gassi, A., Marzorati, S., Di Bartolomeo, P., Gentile, S., Govoni, A., Lovisa, L., Romanelli, M., Ferretti, G., Pasta, M., Spallarossa, D. and Zunino, E. (2005), Mainshocks and aftershocks of the 2002 molise seismic sequenze, southern Italy, *J. Seismol.*, **9**, 487-494.

Basili, R., and Vannoli, P. (2005). Source ITGG052 *San Giuliano di Puglia* and Source ITGG053 *Ripabottoni*. In: DISS Working Group, Database of Individual Seismogenic Sources (DISS), Version 3.0.1: A compilation of potential sources for earthquakes larger than M 5.5 in Italy and surrounding areas. http://www.ingv.it/DISS/ - Istituto Nazionale di Geofisica e Vulcanologia.

Maffei, J. and Bazzurro, P. (2004), The 2002 Molise, Italy, Earthquake, *Earthquake Spectra,* **20-S1**, S1-S22.

Nuti, C., Santini, S. and Vanzi, I. (2004), Damage, Vulnerability and Retrofitting Strategies for the Molise Hospital System Following the 2002 Molise, Italy, Earthquake, *Earthquake Spectra,* **20-S1**, S285-S299.

Pacor, F., Cultrera, G., Mendez, A. and Cocco, M. (2005), Finite Fault Modeling of Strong Motion Using a Hybrid Deterministic-Stochastic Approach, *Bull. Seism. Soc. Am.*, **95**, 225-240.

Satoh, T. (2002), Empirical Frequency-Dependent Radiation Pattern of the 1998 Miyagiken-Nanbu Earthquake in Japan, *Bull. Seism. Soc. Am.*, **92**, 1032-1039.

Spudich, P. and Frazer, L.N. (1984), Use of ray theory to calculate high frequency radiation from earthquake sources having spatially variable rupture velocity and stress drop, *Bull. Seism. Soc. Am.*, **74**, 2061-2082.

SSN – Dipartimento della Protezione Civile – Ufficio Servizio Sismico Nazionale – Servizio Sistemi di Monitoraggio (2004), The Strong Motion Records of Molise Sequence (October 2002 – December 2003), *CD-ROM*, Rome, 2004.

Valensise, G., Pantosti, D. and Basili, R. (2004), Seismology and Tectonic Setting of the 2002 Molise, Italy, Earthquake, *Earthquake Spectra,* **20-S1**, S23-S37.

Vallée, M. and Di Luccio, F. (2005), Source analysis of the 2002 Molise, southern Italy, twin earthquakes (10/31 and 11/01), *Geophys. Res. Lett.,* **32**, L12309.

Wells, D.L. and Coppersmith, K.J. (1994), New Empirical Relationships among Magnitude, Rupture Length, Rupture Width, Rupture Area, and Surface Displacement, *Bull. Seism. Soc. Am.*, **84**, 974-1002.

Zeng, Y., Anderson, J. G. and Yu, G. (1994), A composite source model for computing realistic synthetic strong ground motions, *Geophys. Res. Lett.*, **21**, 725-728.